NURETH14-022

# DEVELOPMENT OF A COUPLED 1D-3D THERMAL-HYDRAULIC CODE FOR NUCLEAR POWER PLANT SIMULATION AND ITS APPLICATION TO A PRESSURIZED THERMAL SHOCK SCENARIO IN PWR

**A. Papukchiev, G. Lerchl, J. Weis, M. Scheuerer and H. Austregesilo**
Gesellschaft fuer Anlagen- und Reaktorsicherheit (GRS) mbH, Garching, Germany

## Abstract

Thermal-hydraulic (TH) system codes are developed for the evaluation and improvement of the design and safety of nuclear facilities. Since the numerical modeling of the thermal-hydraulic processes is 1D in nature, these programs have only limited capabilities to predict in detail 3D flows and coolant mixing processes. In contrast, computational fluid dynamics (CFD) software tools are used for 3D flow calculations with high spatial resolution. In order to realistically and efficiently simulate the thermal-hydraulic phenomena in a nuclear power plant (NPP), GRS has developed a methodology for the coupling of the TH system code ATHLET with the 3D CFD software ANSYS CFX. Within the European project NURISP validation activities for the 1D-3D code ATHLET - ANSYS CFX based on a Pressurized Thermal Shock (PTS) related experiment are performed.

## Introduction

TH system codes are being successfully used in the last decades for the analyses of the physical behavior of NPPs under off-normal or accidental conditions to evaluate and improve the design, operation and safety of current nuclear installations. These codes are extensively validated against experiments and provide reliable results at comparatively low computational cost. Nevertheless, such programs use simplifications in the mathematical models describing the simulated systems. Balance equations for mass, momentum and energy for the two phases are obtained by averaging local basic flow equations over coarse meshes in space and solved in 1D direction. As a result, mean values for relevant physical parameters are calculated which in reality are spatially distributed fields. However, for specific nuclear reactor safety problems with well pronounced 3D mixing effects, like boron dilution, pressurized thermal shock, and main steam line break, a high spatial resolution and 3D flow modeling is needed.

CFD codes are capable to predict three-dimensional fluid flow behavior in complex geometries and can provide detailed distributions of the physical parameters in space and time. Such programs are already widely used in the oil, automotive, power generation, marine, aviation and other industries. Unfortunately, CFD simulations require very high computation time so that a full CFD representation of the primary circuit of a NPP is currently not feasible. Therefore, stand-alone 3D CFD simulations are performed only for certain parts of the primary circuit where 3D phenomena occur (e.g. the downcomer).

In order to perform advanced best-estimate analyses and overcome the deficiencies of CFD and system codes at the same time, a direct coupling of these simulation tools is pursued. A new methodology for the coupling of the GRS TH system code ATHLET with the commercial CFD software package ANSYS CFX is currently being developed at GRS. Main efforts are related to the implementation of explicit and semi-implicit schemes, to the simulation of different test configurations as well as to the validation on large scale experiments.

First verification calculations have already been presented in [1]. Within the framework of the European Nuclear Reactor Integrated Simulation Project (NURISP), ATHLET - ANSYS CFX validation activities for the simulation of pressurized thermal shock phenomena are being carried out. The selected experiment was performed within the OECD/NEA Rig of Safety Assessment (ROSA) project in the Japanese Large Scale Test Facility (LSTF) and deals with flow mixing and temperature stratification during emergency coolant injection in the primary circuit of a pressurized water reactor (PWR). The main objective of this study is to validate the ATHLET - ANSYS CFX coupling methodology.

# 1. Code extensions

The first activities related to the ATHLET - ANSYS CFX coupling have been carried out in close collaboration between GRS and ANSYS Germany [2]. The coupling methodology was then further developed at GRS. The next paragraphs give a brief description of the code modifications and boundary exchange parameters.

## 1.1 Extension of the system code ATHLET

In order to prepare the system code for the coupling with ANSYS CFX, several major modifications were performed by ATHLET developers [3]. Now ATHLET can be called as a subroutine by ANSYS CFX to selectively perform different run sequences (program initialization and reading of input data, start of steady state calculation, etc.) controlled by a key parameter. In hydraulically coupled codes, one of the programs provides scalar variables (pressure, fluid temperature, quality, etc.) and the other calculates vector variables (mass flow or velocity and related temperature, etc.) at the coupling point. To provide stable boundary conditions for both 1D and 3D domains, these coupling options are alternately utilized. Therefore, two coupling options for the data exchange in single phase thermal-hydraulic problems have been developed within ATHLET (Fig. 1):

*Option 1:* ATHLET provides fluid velocity and temperature and receives pressure and temperature from ANSYS CFX.

*Option 2:* ATHLET provides pressure and temperature and receives mass flow rate and fluid temperature from ANSYS CFX.

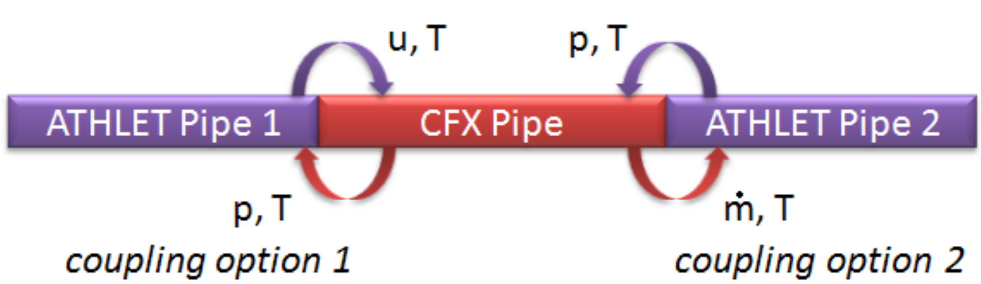


Figure 1: Thermal-hydraulic exchange parameters.

### 1.2 Extension of the CFD program ANSYS CFX

The ANSYS CFX coupling technology is based on a more general framework which has already been established in ANSYS CFX for coupling purposes with other 1D codes. For the ATHLET - ANSYS CFX project, major modifications in ANSYS CFX were related to the extension of its input deck definitions and the utilization of the shared library which contains the coupling interface and the ATHLET code. Another important modification is related to the calling sequence of the routine which executes ATHLET.

## 2. Coupling schemes

Coupling schemes can be categorized by the type of applied solution algorithm as explicit, semi-implicit and fully implicit coupling schemes. In typical explicit coupling, the data exchanged between the codes remains constant during the time step advancements. In the implicit coupling, the interdependency of the own and coupling solution variables must be known in each code, i.e. through the calculation of a coupling Jacobian matrix. Semi-implicit coupling schemes are generally based on recalculation of the executed time step with both codes several times until a converged solution is found. For ATHLET – ANSYS CFX, explicit and semi-implicit coupling schemes have been developed. More information is given in [4].

### 2.1 Explicit coupling scheme

In this coupling strategy, the data is exchanged only at the end of the synchronization time interval $\Delta T$ (Fig. 2, left). A time step is performed by the CFD program providing new coupling variables to ATHLET. With the new boundary conditions, the system code calculates the same $\Delta T$ and returns its results to ANSYS CFX which continues with the next time step. Explicit coupling schemes are easier to implement in comparison to the semi-implicit ones. They can produce reliable results at reasonable CPU times. Exchanging thermal-hydraulic data only after the closure of the time step is beneficial in terms of CPU time, and, at the same time, penalizing for the simulation stability in certain cases. Moreover, the time step size is limited by the Courant-Friedrich-Levy limit [5].

### 2.2 Semi-implicit coupling scheme

The main idea behind the semi-implicit scheme is that both programs repeat the current time step several times with updated boundary conditions in an iterative manner until specified convergence criteria are reached (Fig. 2, right). At that point, ANSYS CFX closes the time step and initiates the next one. With such a strategy, consistent thermal-hydraulic solution parameters in both the system code and CFD domains are achieved. Large increments of the thermal-hydraulic parameters within one time step in one of the domains (1D or 3D) are limited by the immediate feedback from the respective thermal-hydraulic parameter in the other domain. This allows larger time steps and leads to improved numerical stability which is, in fact, the most important advantage of this type of coupling.

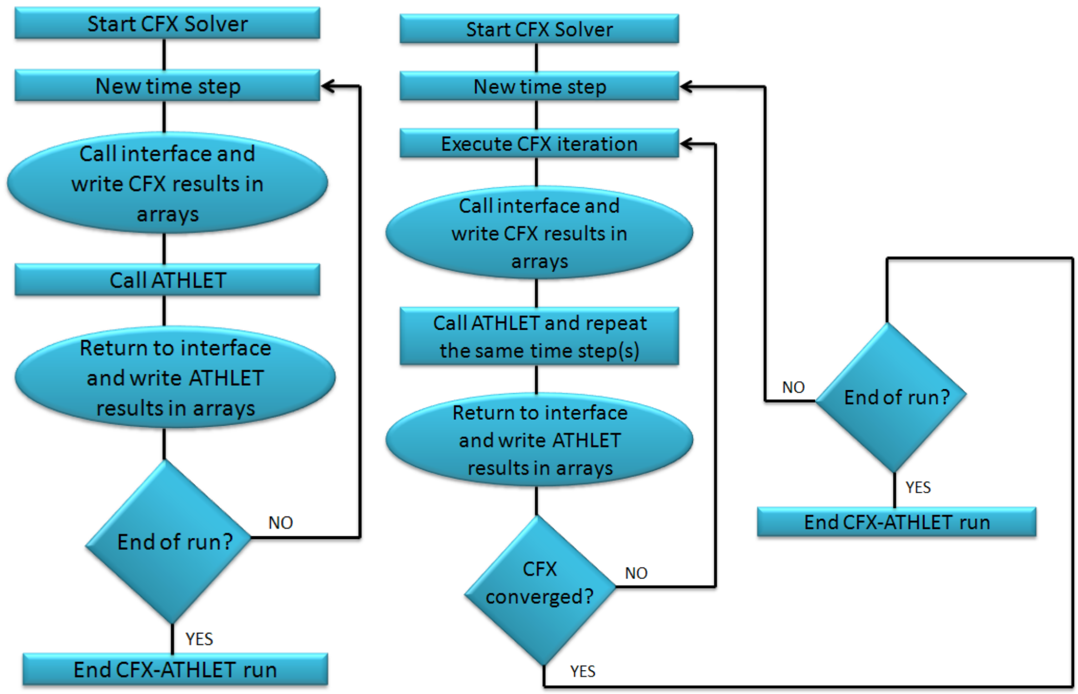


Figure 2: Explicit (left) and semi-implicit (right) coupling schemes.

## 3. Large Scale Test Facility and OECD ROSA V Test 1-1 experiment

The Japanese LSTF represents a four-loop, 3423 MW thermal power Westinghouse PWR by a full-height and 1/48 volumetrically-scaled two-loop system [6]. The cold legs are similar, and consist of straight and elbow parts which are attached to the main coolant pumps (Fig. 3). However, the emergency core cooling (ECC) injection nozzles in the cold legs differ in shape and location. ECC Nozzle A is perpendicular to the main pipe simulating VVER reactor type conditions, while ECC Nozzle B forms a 45° angle with the cold leg.

The Test 1-1 was performed in 2006 within the frame of OECD/NEA project ROSA V. The goal of the experiment was to investigate flow mixing and temperature stratification under natural circulation conditions, and to provide data for the validation of computer codes. Temperatures were measured with thermocouple rakes in the cold legs below the injection nozzle (TE1), and at two cross-sectional planes between the injection nozzle and the downcomer (TE2, TE3), see Fig. 4. Each rake in the cold leg consists of 21 thermocouples positioned in three columns and seven rows (Fig. 7). Additionally, 18 thermocouples were installed in the downcomer below the cold legs (TE4).

The experiment started with forced circulation and when the pumps were switched off, natural circulation at 15.5 MPa and 2% core power established in the primary circuit. The simulation results presented in this paper are focused only on the first phase of Test 1-1, where ECC water was injected for about 110 s in the cold leg A at these conditions. The temperature difference between the hot water in the primary system and the cold ECC water is almost 250 K resulting in density differences greater than 200 kg/m$^3$.

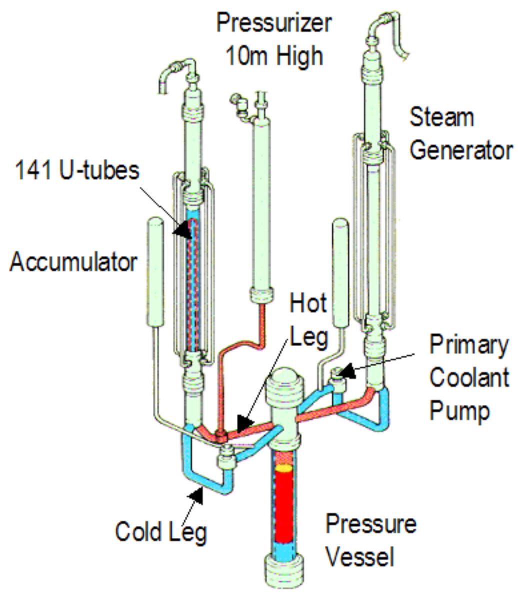


Figure 3: Large Scale Test Facility.

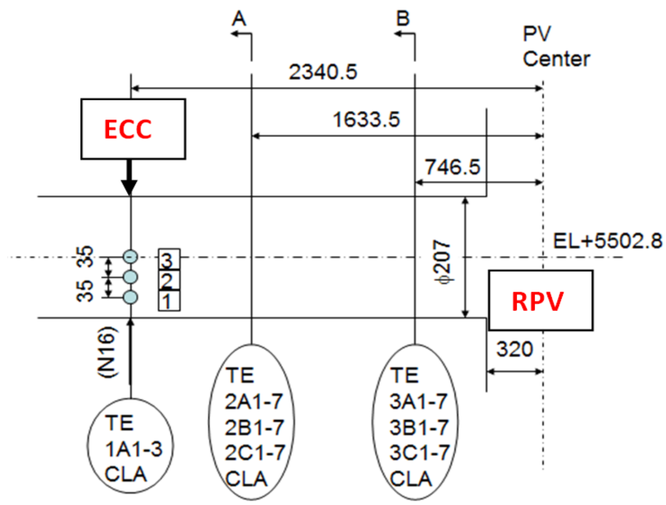


Figure 4: Measurement rakes in cold leg A.

## 4. Pressurized thermal shock simulations

Pressurized thermal shock may occur when cold water is injected in the primary circuit filled with hot coolant. The cold water may rapidly cool down the reactor pressure vessel (RPV) wall when entering the downcomer. This greatly increases the potential for RPV failure by cracking. The cool down process can be even intensified by a thermal stratification in the cold leg. Thermal stresses are more dangerous for the RPV downcomer compared to the cold leg structures because of its thick walls and the presence of welds. Due to the 3D nature of the stratification and mixing phenomena, such reactor safety problems need to be simulated with advanced 3D CFD tools. This experiment is challenging for any thermal-hydraulic program and even more for coupled codes because strong buoyancy and mixing effects in natural circulation conditions have to be addressed in a proper manner. Next paragraphs describe the simulation setups, while final results are discussed in chapter five.

### 4.1 Initial and boundary conditions

In this work, three different simulations were performed – ATHLET stand alone, ANSYS CFX stand alone and a coupled ATHLET – ANSYS CFX calculation. The transient ANSYS CFX stand-alone and the coupled calculations were started from a steady-state solution of the natural circulation part of ROSA Test 1-1, while ATHLET stand-alone calculations involved also the simulation of the transition from forced to natural circulation in LSTF. For the CFD stand-alone simulations, time-dependent, measured mass flow rates and temperatures were specified at the inlet boundaries. Since the pump wheel was not modeled, its influence on the flow at the inlet of the cold leg A was not considered in the CFD and coupled calculations. At the outlet, a constant pressure boundary condition was prescribed and at the walls, no-slip boundary conditions for smooth surfaces were used.

In the coupled 1D-3D calculations the transient mass flow rates and temperatures were calculated by ATHLET – ANSYS CFX, because in this case the thermal-hydraulic configuration is not open system (like the stand-alone CFD calculations with the cold leg A), but a closed system representing the complete LSTF. Table 1 shows the initial values of the main thermal-hydraulic parameters. Further parameters can not be provided, since the ROSA V experimental data are restricted.

Table 1: Initial conditions.

| Parameter | Initial value |
|---|---|
| Fluid temperature at pump exit | 553.7 [K] |
| Mass flow rate at pump exit | 5.9 [kg/s] |
| Fluid density at pump exit | 764 [kg/m3] |
| Fluid velocity at pump exit | 0.24 [m/s] |
| Pressure at cold leg outlet | 15.5 [MPa] |

## 4.2 1D simulations with the system code ATHLET

For the 1D system code calculations, the existing, detailed 1D ATHLET input deck for the LSTF was used. Both loops A and B were modeled and connected to a RPV with two-channel downcomer and core representation. The pressurizer has been simulated with five nodes and connected via the surge line to the hot leg of loop A. Fine nodalization scheme with three different heat exchanger U-tube bundles (short, medium and long) has been developed for the modeling of the steam generators (Fig. 5). The secondary side is also modeled in detail. With this input deck several ATHLET stand-alone calculations have been performed not only for the single phase, but also for the two-phase part of Test 1-1. The calculated averaged thermal-hydraulic parameters were in good agreement with experimental data.

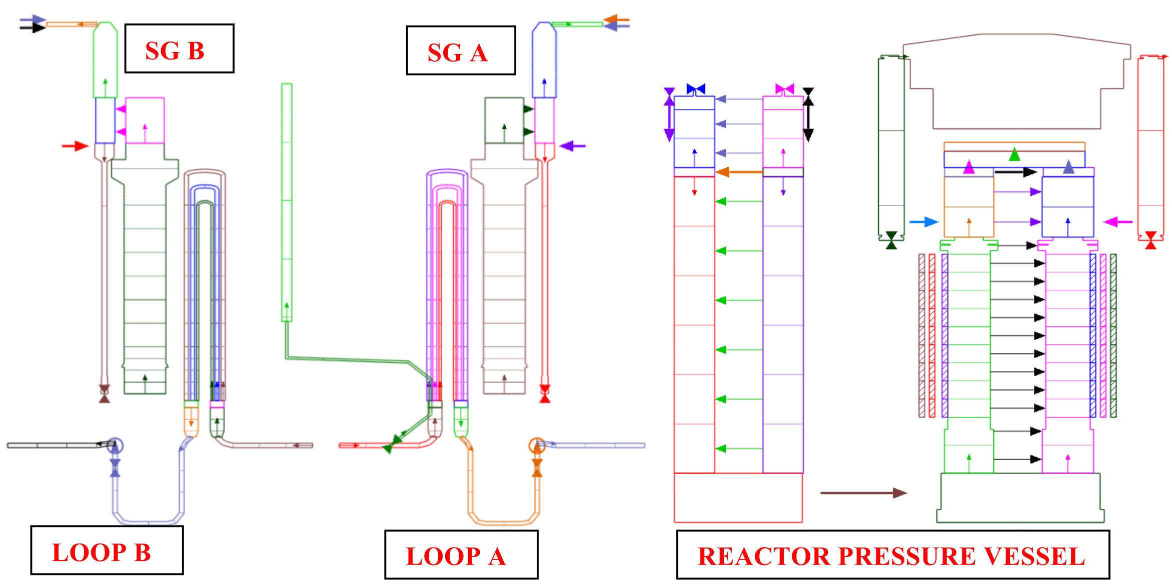


Figure 5: ATHLET model of LSTF.

### 4.3 3D simulations with the CFD program ANSYS CFX

#### 4.3.1 Grid generation

A CAD model of the cold legs, the ECC lines, and the downcomer was generated on the basis of the available drawings. This geometry served as an input for the ICEM CFD software, which has been used to prepare systematically refined hexahedral grids. Careful grid sensitivity studies were performed in accordance with the OECD/NEA Best Practice Guidelines [7], and a fine grid with 5.2 million elements has been selected for the first 3D simulations [8].

Since the main objective of this coupling study was to validate the ATHLET-ANSYS CFX coupling methodology and to investigate the thermal stratification in the cold leg A, it was decided to accelerate the calculations by “cutting” the 4 m long section of the LSTF cold leg A between the main coolant pump and the RPV downcomer (which includes the ECC injection nozzle) and to use it for the ANSYS CFX stand-alone and coupled calculations. This part of the cold leg is well instrumented with measurement rakes TE2 (close to the ECC injection) and TE3 (close to the RPV downcomer) which results in 2x21 thermocouples in total. Additional thermocouples are positioned under the ECC injection line (TE1). After small refinement, the final mesh of the cold leg A consisted of 1.13 million elements (Fig. 6). Figure 7 gives an impression how one measurement rake with 21 thermocouples looks like in reality. The geometry of the rakes was not resolved in the numerical grid.

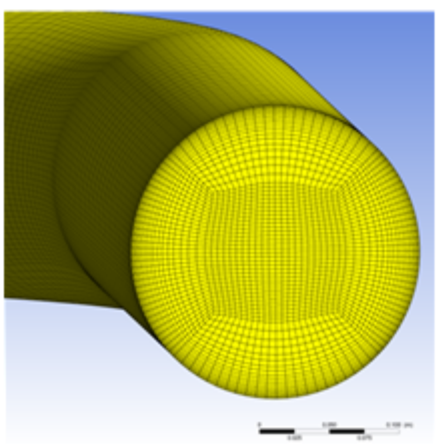

Figure 6: ANSYS CFX grid.

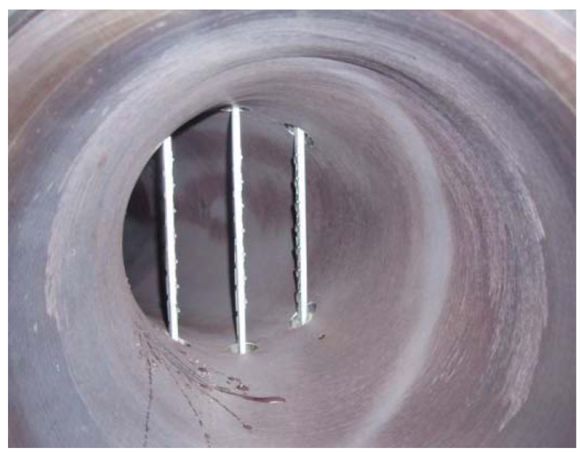

Figure 7: Rake with thermocouples.

#### 4.3.2 Mathematical models

For the correct modeling of the buoyant flows in the LSTF, buoyancy terms in the momentum equation and in the production terms of the turbulence model equations have been included. These are driven by the density difference between the hot and cold water, while water density is calculated as a function of temperature on the basis of IAPWS-IF97 tables [9]. Dynamic viscosity and conductivity of the fluid are also derived from these tables.

Preliminary calculations with two turbulence models were carried out - the Shear Stress Transport (SST) model of Menter [10] and the Baseline Reynolds Stress Turbulence model (BSL RSM) [11].

The simulations with the more complex BSL RSM showed better agreement with experimental data, and therefore it was selected for the coupled 1D-3D calculations. Both models were combined with 'automatic' wall functions in which the near-wall fluxes are derived from either linear or logarithmic wall laws, depending on the position of the wall-adjacent grid point.

In a next step, the numerical and model errors have been assessed. The ANSYS CFX convergence criteria have been set to RMS residual target 1.E-4 and the mass conservation target was set to 1.E-3. A first-order upwind advection scheme was used in the simulations, because the second-order high resolution scheme predicted, as expected, more oscillatory flow behavior. Constant 0.05 s time steps have been selected for both ANSYS CFX stand-alone and the coupled ATHLET - ANSYS CFX calculations.

## 4.4 Coupled 1D-3D simulations with ATHLET - ANSYS CFX

For the simulations with ATHLET - ANSYS CFX, a coupled 1D-3D model of the LSTF has been developed. In the first step, the 1D ATHLET pipe section in the cold leg A between the main coolant pump and the RPV downcomer, was "replaced" with the same 3D ANSYS CFX pipe section (as described in chapter 4.3.1). For this purpose, coupling options 1 and 2 were used and the thermal-hydraulic parameters shown in Fig. 1 were exchanged between the programs after each time step. The ATHLET - ANSYS CFX model of the LSTF can be seen in Fig. 8. In this way, the part of the primary circuit with relevant 3D effects (cold leg A) is treated with ANSYS CFX, and ATHLET is used to provide fast solution for the flow behavior in those areas where 1D simulation is adequate. The coupled calculation was started two seconds before the injection of the cold water in order to allow both codes to find a stable solution for the natural circulation conditions. The ATHLET and ANSYS CFX input deck setups were identical to the ones used in the stand-alone calculations.

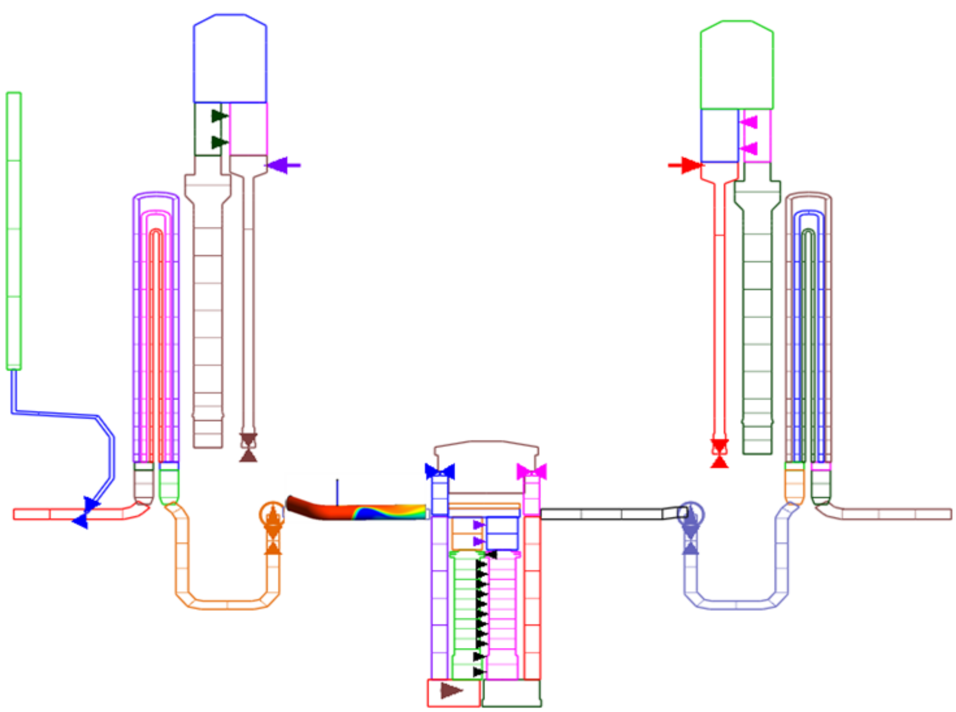

Figure 8: ATHLET – ANSYS CFX model of the LSTF RPV and loop A.

## 5. Analysis and comparison of the simulation results with experimental data

The 3D CFD and the coupled 1D-3D calculations were performed with the ANSYS CFX software (Version 11) and ATHLET Mod. 2.2 Cycle A. These were run on eight Intel Woodcrest 3.0 GHz CPUs integrated in a Sun Blade X6250 cluster system. Both ANSYS CFX and ATHLET - ANSYS CFX calculations of 125 s transient time and 0.05 s time step size run approximately five days. In the coupled simulations, ATHLET CPU time is so small that it can be neglected.

In the first step of the comparative analysis, the results from the performed coupled 1D-3D simulations were visualized with the help of ANSYS CFX Post software. Figure 9 shows the calculated temperature distribution during ECC injection at the wall (left picture) of the cold leg A and its central longitudinal section (right picture). The vertically downwards injected cold ECC water hits the bottom of the cold leg and then swashes to the left and right pipe walls. Due to its higher density, the cold water pushes the lighter hot water to the top and gradually stratifies at the bottom of the cold leg. This can be also observed in Fig. 10 which shows the temperature distribution in the cross-section planes 0.45 (top, left), 0.90 (top right), 1.35 (bottom left) and 1.80 m (bottom right) from the ECC injection nozzle in the direction of the RPV inlet. One sees that horizontally shaped and stratified temperature layers build approx. 0.3 m away from the RPV entrance (bottom right picture). The maximum temperature difference between top and bottom of the pipe in this cross-section is 12 K.

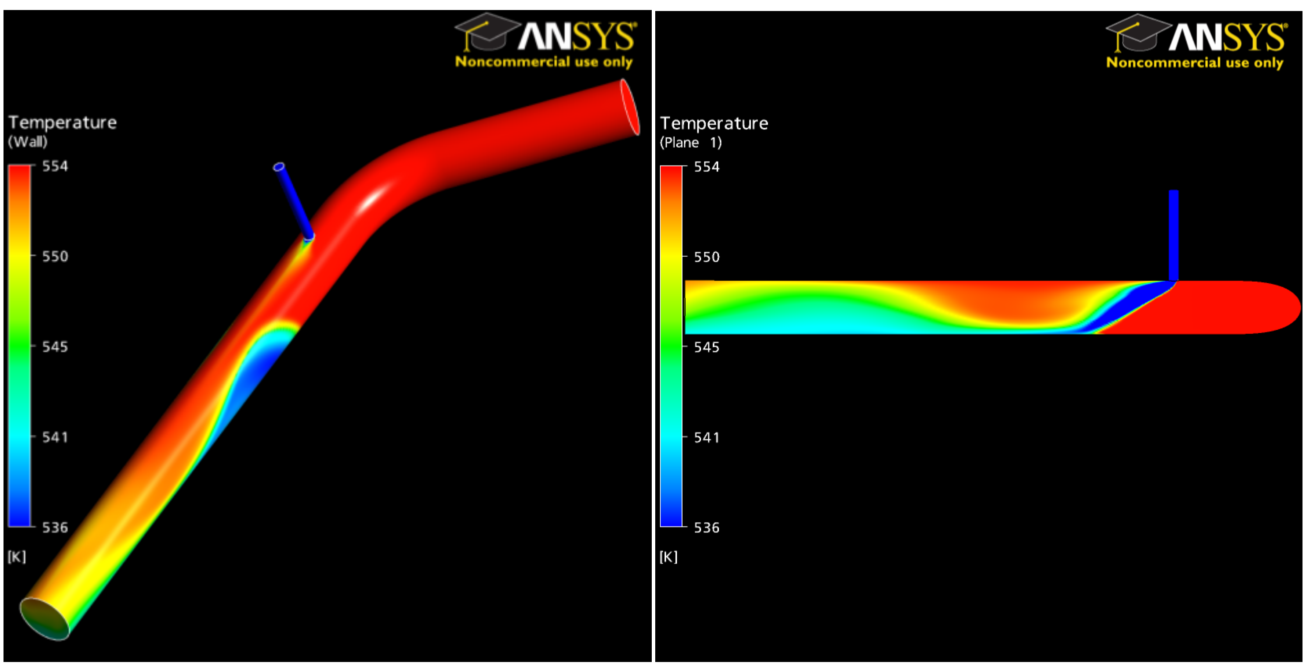


Figure 9: Calculated temperature distribution in the cold leg A.

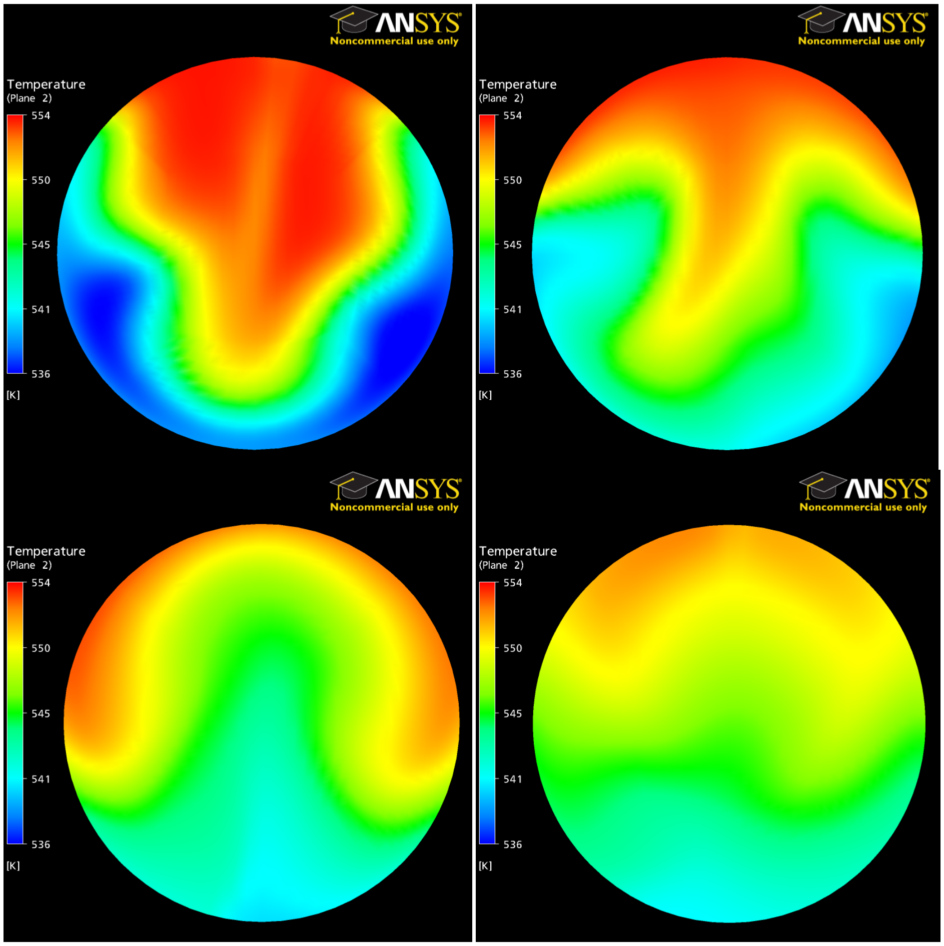


Figure 10: Temperature distribution 0.45 (top left), 0.90 (top right), 1.35 (bottom left) and 1.80 m (bottom right) from the ECC injection nozzle.

Figures 11 shows the comparison to data for the thermocouple TE1205 (rake TE3) which is situated centrally at the bottom of the cold leg A, 1.59 m from the ECC injection nozzle (Fig. 4). Since the OECD ROSA data are restricted, no absolute numbers can be shown. Nevertheless, one still can see the very good agreement between experiment and calculation with the help of the absolute measurement uncertainty. Generally, most of the results in the measurement rake TE3 compare good to the experimental data.

Thermocouple TE1184 is located at the same bottom position (like TE1205), but in the TE2 measurement rake, which is situated just 0.7 m away from the ECC injection nozzle. In this case the distribution of the cold water in the pipe cross-section is not predicted correctly by the code and the temperature in the bottom part of the cold leg A is higher than the measured one (Fig. 12).

There are several possible reasons for the large deviations in the TE2 measurement rake. The first one is that the experimental flow might be influenced by the relatively large fixtures of the thermocouples (Fig. 7) which have not been modeled. Another reason could be inadequate turbulence modeling. Measurement rake TE2 is close to the location where the cold ECC water jet impinges on the bottom of cold leg A. In this area, not only mixing phenomena but also strong buoyancy effects due to the large density differences between both streams (>200 kg/m$^3$) come into play. This might be too challenging for the two-equation and RSM turbulence models.

Another question is related to the fact that good agreement between experiment and calculation is found in TE3 measurement rake (downstream), although these results are affected by the temperature distribution in TE2 (upstream), which was not predicted correctly by the CFD code. One should not forget, that both fluids mix and downstream the temperature distribution over the pipe cross section gets more and more homogeneous (compare the first and the last picture in Fig. 10). Sharp density and temperature gradients are not longer present and the correct prediction of the fluid temperature is not that challenging for the RSM turbulence model.

At the moment, extensive, high resolution Large Eddy Simulation (LES) is being performed at GRS which will help to identify the reason for the poor agreement at TE2 rake. LES is a family of methods that resolve large-scale eddies in the flow equation solution, and uses sub-grid scale turbulence models for the small-scale eddies [7]. To perform the LES Smagorinsky calculation, a very fine mesh with 7.2 million elements, generated on the same CAD model (no measurement fixtures) is used. This strategy will help to separate the geometry modeling from the turbulence modeling effects.

Figure 13 compares ATHLET stand-alone and coupled ATHLET - ANSYS CFX results for the average pipe cross-section temperatures in the ATHLET control volume downstream of the ANSYS CFX domain near the RPV downcomer inlet. The good agreement between ATHLET stand-alone and ATHLET - ANSYS CFX demonstrates that the coupled code system successfully accomplishes the transition from spatially distributed to lumped parameter approximation schemes. The comparison with the measured temperature averaged over 21 thermocouples distributed across the pipe cross section (actually located 0.4 m upstream of the RPV downcomer inlet) shows that the end of the injection phase is predicted slightly better by the coupled codes due to the significantly reduced numerical diffusion.

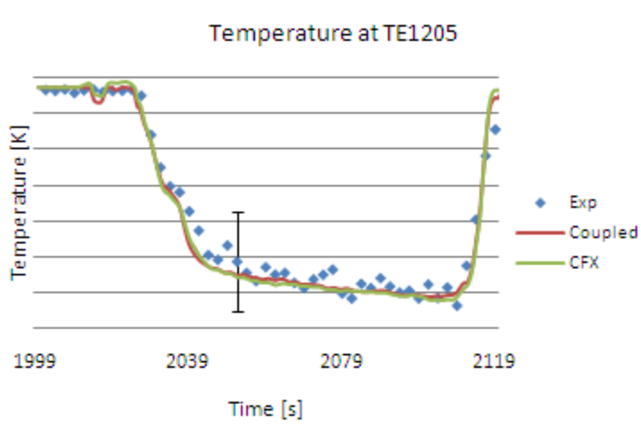


Figure 11: Local temperature at TE1205 (TE3).

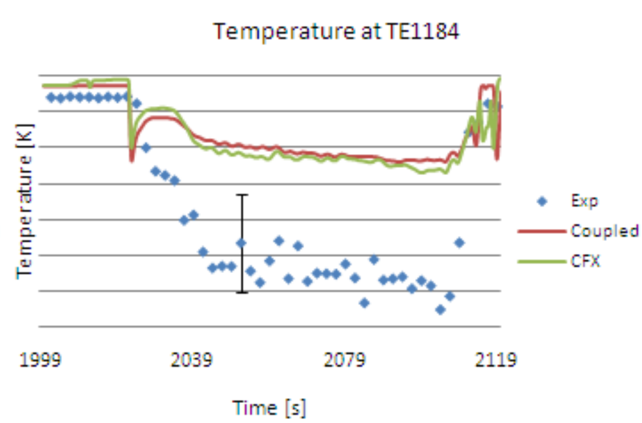


Figure 12: Local temperature at TE 1184 (TE2).

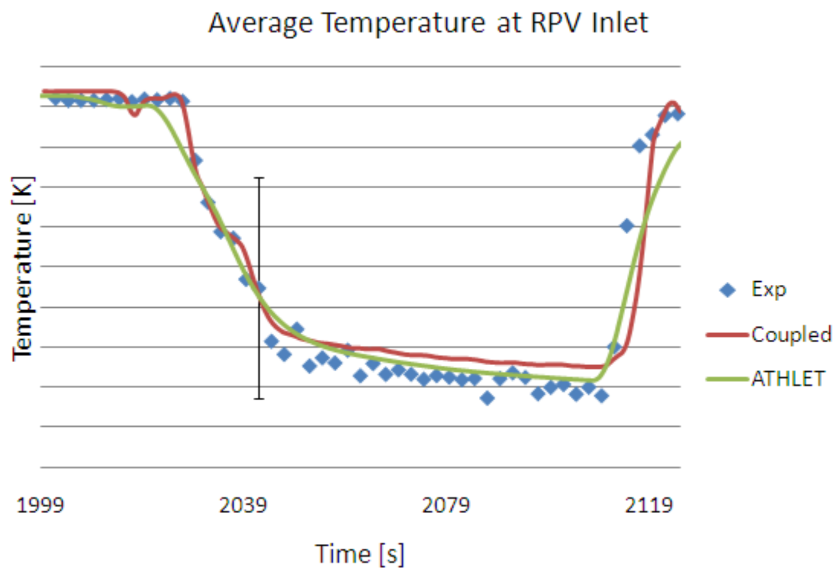


Figure 13: Average temperature at RPV inlet.

The main objective of the presented calculations was to validate the ATHLET – ANSYS CFX coupling methodology. It should be stated, that in both measurement rakes TE2 and TE3 a very good agreement between ANSYS CFX stand-alone and ATHLET - ANSYS CFX calculations was observed. This result proves the consistency of the ATHLET - ANSYS CFX coupling methodology. In a next step, the advantages of the coupled code over the stand alone calculations will be evaluated. A faster transient with strong feedback between the component of interest (3D) and the rest of the nuclear cooling system (1D) will be simulated.

## 6. Conclusion

System codes like ATHLET are based on one dimensional models and these have only limited capabilities to predict in detail 3D flows and coolant mixing processes, being important for certain classes of transients and accidents. In order to overcome these limitations and extend the capabilities of ATHLET, explicit and semi-implicit schemes have been developed and implemented to couple the GRS best estimate code with the commercial CFD tool ANSYS CFX. Within the European project NURISP validation activities for the 1D-3D code ATHLET - ANSYS CFX are being performed for the OECD ROSA V Test 1-1 dedicated to the PTS phenomena in PWR. The comparison with experimental data showed good agreement in the TE3 and larger deviations in the TE2 measurement rake, which is close to the ECC injection nozzle. Possible reasons for these are insufficient geometry modeling or inadequacy of the turbulence models to simulate mixing phenomena in buoyant flows with large density differences. Nevertheless, a very good agreement between stand-alone calculations with ATHLET and ANSYS CFX, and coupled 1D-3D ATHLET - ANSYS CFX calculations has been observed, proving the consistency of the new coupling methodology.

## Acknowledgements

This work was performed within the NURISP project, which was partly funded by the EC in the 7th Euratom Framework Programme (Grant Agreement Number 232124).

## References


[1] A. Papukchiev, G. Lerchl et al., "Extension of the Simulation Capabilities of the 1D System Code ATHLET by Coupling with the 3D Software Package ANSYS CFX", Proceedings of NURETH-13 Conference, Kanazawa, Japan, Sept. 27- Oct. 3, 2009.

[2] Ch. L. Waata and Th. Frank, "Coupling of ANSYS CFX with 1D System Code ATHLET", Final Report, German Federal Ministry for Economy and Technology, Reactor Safety Research Project 1501328, Germany, 2008.

[3] G. Lerchl, "Kopplung von ATHLET mit dem CFD-Programm CFX", Technische Notiz TN-LER-04/07, GRS, 2007.

[4] A. Papukchiev and G. Lerchl G., Development and Implementation of Different Schemes for the Coupling of the System Code ATHLET with the 3D CFD Program ANSYS CFX, Proceedings of the NUTHOS-8 Conference, Shanghai, China, October 10-14, 2010.

[5] W. L. Weaver, E.T. Tomlinson, et al., "A Generic Semi-Implicit Methodology for Use in RELAP5-3D", Nuclear Engineering and Design, 211, pp.13-26, 2002.

[6] JAERI, "ROSA V Large Scale Test Facility (LSTF) System Description for the Third and Fourth Simulated Fuel Assemblies", Tokai Research Establishment, Japan Atomic Energy Research Institute, 2003.

[7] J. Mahaffy, "Best Practice Guidelines for the Use of CFD in Nuclear Reactor Safety Applications", NEA/CSNI/R, 2007.

[8] M. Scheuerer, J. Weis, "CFD Calculations of OECD/NEA ROSA Test 1-1", NURISP Deliverable D2.1.2.4a, GRS, 2010.

[9] W. Wagner, and A. Kruse, "The Industrial Standard IAPWS-IF97: Properties of Water and Steam", Springer-Verlag, Berlin, 1998.

[10] F. R. Menter, "Two-Equation Eddy-Viscosity Turbulence Models for Engineering Applications", AIAA-Journal, Vol. 32, pp. 269 – 289, 1994.

[11] ANSYS CFX Reference Guide, ANSYS CFX Release 11.0, 2006.